Conformation and Dynamics of Bovine Brain S-100a Protein Determined by Fluorescence Spectroscopy†

Chien-Kao Wang,‡ Rajam S. Mani,§ Cyril M. Kay,§ and Herbert C. Cheung*,‖

Department of Physiology and Biophysics, University of Washington, Seattle, Washington 98195, MRC Group in Protein Structure and Function, Department of Biochemistry, University of Alberta, Edmonton, Alberta T6G 2H7, Canada, and Department of Biochemistry, University of Alabama at Birmingham, Birmingham, Alabama 35294

Received December 19, 1991; Revised Manuscript Received February 24, 1992

ABSTRACT: We have used time-resolved laser fluorescence spectroscopy to investigate the intensity and anisotropy decays of the single tryptophan residue in bovine brain S-100a ($\alpha\beta$) protein. The steady-state and acrylamide quenching results indicated that the Trp 90 of the α-subunit was partially buried in a relatively nonpolar environment at pH 7.5. Both Ca^{2+} and pH 8.5 slightly enhanced the exposure of the residue to the solvent, but the residue remained partially buried in the calcium complex at both pH values. The best representation of the intensity decays was a linear combination of three exponential terms, regardless of solvent condition and temperature. The three lifetimes (τ_i) were in the range of 0.4–5 ns and insensitive to emission wavelength, but their fractional amplitudes (α_i) shifted in favor of the shortest component (α_1) when the decays were measured at the blue end of the emission spectrum. These results suggest that an excited-state interaction between the indole ring and the side chain of an adjacent residue may be responsible for the observed shortest lifetime. In the presence of Ca^{2+}, the three lifetimes remained relatively unaltered, but the values of α_1 decreased by a factor of 2.3 at pH 7.2 and a factor of 1.8 at pH 8.2. This Ca^{2+}-induced decrease may be attributed to disruption of the putative excited-state interaction resulting from reorientations of the α-helical segments flanking a Ca^{2+}-binding loop (residues 62–73). At both pH 7.2 and 8.4, the anisotropy decays of the apoprotein followed a biexponential decay law. The anisotropy recovered at zero time was in the range of 0.221–0.261, suggesting the existence of some very fast motion of the tryptophan side chain not resolvable in the present experiments. The two recovered correlation times were $\theta_1 = 1$ ns and $\theta_2 = 16$ ns at the neutral pH, and $\theta_1 = 1$ ns and $\theta_2 = 18$ ns at the alkaline pH. The addition of Ca^{2+} at pH 7.2 had no effect on θ_1 but increased θ_2 by over 5 ns. However, Ca^{2+} at pH 8.4 changed the anisotropy decay to monoexponential, eliminating θ_1 and decreasing θ_2 to 16 ns. These results provide additional evidence of a difference in the conformation of S-100a at the two pH values. The long correlation times are compatible with an axial ratio in the range of 4–5 for the apoprotein at pH 7.2 and suggest a more asymmetric hydrodynamic shape for the Ca^{2+} complex. This work has yielded time-resolved fluorescence results to characterize the effect of Ca^{2+} binding on both localized and global conformations of S-100a protein.

The highly acidic water-soluble S-100 protein (Moore, 1965) was originally considered to be a nervous system specific protein found primarily in the cytosol of glial cells (Ludwin et al., 1976). However, in recent years many authors have reported the presence of S-100 antigens in non-nervous tissues such as skin (Cocchia et al., 1981), chondrocytes (Stefansson et al., 1982), and T-lymphocytes (Kanamori et al., 1982). The exact biological function of S-100 protein is not known, but the fact that it is found in the brain of both invertebrates and vertebrates with a constant immunological response (Moore, 1973) indicates that it has been conserved throughout evolution and hence may have an important role in the function of the nervous system.

S-100 protein is composed of three components, S-100a_0, S-100a, and S-100b with subunit composistion $\alpha\alpha$, $\alpha\beta$, and $\beta\beta$, respectively. The amino acid sequence of S-100 protein indicates that there is extensive homology (58%) between the α- and β-subunits (Isobe & Okuyama, 1981). The α- and β-subunits consist of 93 and 91 amino acid residues, respectively, and the α-subunit is characterized by the presence of a single tryptophan residue at position 90. Each of the subunits contains one Ca^{2+}-binding site at the C-terminus, similar to the EF model in parvalbumin (Tufty & Kretsinger, 1975). In addition, at pH 8.4, another Ca^{2+}-binding site becomes available, presumably at the N-terminus, resembling the I–II domains of bovine intestinal Ca^{2+}-binding protein as described by Szebenyi et al. (1981).

S-100 proteins undergo a conformational change in the presence of Ca^{2+} (Mani et al., 1982; Mani & Kay, 1983, 1985). In the case of S-100a, calcium binding results in exposing the single tryptophan residue to the solvent as revealed by UV-difference spectroscopy (Mani & Kay, 1983, 1987). In the present study, the fluorescence intensity and anisotropy decays of the single tryptophan in bovine brain S-100a protein were determined using pulsed-picosecond laser systems. The effects of Ca^{2+}-binding on the conformation of the protein was studied at two pH values, 7.2 and 8.4. The observed data indicate that the binding of calcium ion induces a conformational change in the protein, whereby the single tryptophan residue has increased solvent accessibility relative to the apoprotein but is still partially buried. The data further suggest differences in the localized and global conformations of the protein between the two pH values.

Materials and Methods

Protein Preparation. S-100a protein was prepared from bovine brain as previously described (Mani & Kay, 1983). The

† This work was generously supported by the Medical Research Council of Canada (C.M.K.) and the Alberta Heart and Stroke Foundation (C.M.K.) and by the U.S. National Institutes of Health, Grant AR25193 (H.C.C.).

‡ University of Washington.
§ University of Alberta.
‖ University of Alabama at Birmingham.

0006-2960/92/0431-4289$03.00/0

purity of the preparation was confirmed by $NaDodSO_4$–polyacrylamide gel electrophoresis. An absorbance of 5.4 at 278 nm for a 10 mg/mL solution was used to determine protein concentration. Prior to fluorescence measurements, the protein was first dialyzed against 25 mM Tris[tris(hydroxymethyl)aminomethane] at the desired pH in the presence of 1 mM EGTA [ethylene glycol bis(β-aminoethyl ether)-*N,N,N',N'*-tetraacetic acid], followed by a second dialysis in the same buffer without EGTA (in the presence of Chelex-100 resin). When cations were present, $MgCl_2$ and $CaCl_2$ were added to 5 and 2 mM, respectively.

Steady-State Fluorescence Measurements. Steady-state fluorescence measurements were carried out on a SLM 8000C photon-counting spectrofluorometer. Spectral measurements were made with 295-nm excitation, and emission spectra were corrected for solvent background and Raman scattering. For measurements of fluorescence quenching by acrylamide, aliquots of a 6 M acrylamide were added to the protein contained in a cuvette, and the emission intensity was determined at 360 nm. The observed intensity was corrected for dilution effect and inner filter effect due to the absorbance of acrylamide at the excitation wavelength. The quenching data were analyzed by the Stern–Volmer equation

$$F_0/F = (1 + K_{SV}[Q])\exp(V[Q]) \quad (1)$$

where F_0 and F are the intensity in the absence and presence of acrylamide, K_{SV} and V are the dynamic and static Stern–Volmer quenching constants, and [Q] is the molar concentration of acrylamide.

Measurements of Fluorescence Intensity Decay. The intensity decay of the single tryptophan in S-100a protein was measured with two different instruments using the single-photon counting techniques (O'Connor & Phillips, 1984). The instrument located at the University of Alabama at Birmingham was equipped with a frequency-doubled, cavity-dumped rhodamine 6G dye laser (Spectra Physics Model 375) which was synchronously pumped by a mode-locked argon ion laser (Spectra Physics Model 171). The dye laser was cavity-dumped at 800 kHz, and the output of the dye laser near 590 nm was frequency-doubled by an angle-tuned KDP crystal to provide pulses at 295 nm for excitation. The emission was isolated at a right angle to the excitation beam with a Schott 0–54 cut-off filter and under rotation-free conditions with a polarizer oriented at the magic angle of 54.7° relative to the excitation direction and was detected by a Hamamatsu R955P PM tube. The time-to-pulse-height converter (TAC) (Ortec model 457) was operated in a conventional configuration, with the voltage ramp being initiated by a signal from the fundamental laser pulse and terminated by the signal from the photomultiplier. Pulse pile-up effects were avoided by ensuring that the ratio of laser pulses to the detected emission photons was greater than 100. The data from the TAC were stored in a Tracor Northern TN-7200 multichannel analyzer (MCA) using 1024 channels for each set of data with a width of 20 ps/channel and were subsequently analyzed in a personal computer. The second picosecond fluorometer used in this work was located at the University of Oregon (Ruggiero & Hudson, 1989) and was equipped with a cavity-dumped dye laser synchronously pumped by a mode-locked Nd:YAG solid-state laser and a Hamamatsu R1294U microchannel plate photomultiplier as the detector. This instrument was used to measure intensity and anisotropy decays isolated with a 360-nm interference filter (band-pass, 10 nm) with excitation at 300 nm.

Measurements of Fluorescence Anisotropy Decay. For anisotropy decay measurements, the excitation light was vertically polarized, and the intensity of the emitted light polarized in the vertical [$I_\parallel(t)$] and horizontal [$I_\perp(t)$] directions was alternately collected in a series of 60-s cycles. This protocol minimized the drift effects of both the lasers and the electronics. The channel width for these measurements was also 20 ps. In a typical experiment, 20000 photon counts were collected in the peak channel for $I_\parallel(t)$, and the $I_\perp(t)$ component was counted for the same period of time as for $I_\parallel(t)$. The time-dependent anisotropy $r(t)$ was calculated from the difference and sum curves generated from the two decay components:

$$r(t) = \frac{I_\parallel(t) - GI_\perp(t)}{I_\parallel(t) + 2GI_\perp(t)} \quad (2)$$

The correction factor G to account for optical differences in the collection of the two polarized decay components was determined by collecting vertically and horizontally polarized components for equal lengths of time with excitation polarized in the horizontal direction. The ratio of the integrated intensities of the two components was the G factor.

Analyses of Decay Data. Intensity decay parameters were recovered from the observed decay curves by using nonlinear least-squares iterative reconvolution procedures with the Marquardt algorithm (Marquardt, 1963; Grinvald & Steinberg, 1974). The intensity decay curves were fitted to a linear combination of exponential terms

$$I(t) = \sum_{i=1}^{n} \alpha_i \exp(-t/\tau_i) \quad (3)$$

where α_i are the amplitudes associated with the lifetimes τ_i. An additional amplitude term was included in the fitting function to correct for scattering. The goodness of a fit between the observed data and the chosen function was evaluated by the following statistics: the weighted residuals, the autocorrelation function of the residuals, the reduced chi-squares ratio (χ_R^2), the Durbin–Watson number (Durbin & Watson, 1951; Lampert et al., 1983), and the runs test (Gunst & Mason, 1980). The Durbin–Watson (D–W) number examines the correlation of the residual values in neighboring channels. The following D–W values are considered adequate for the number (i) of exponential terms in the function: $i = 1$, D–W > 1.7; $i = 2$, D–W > 1.75; and $i = 3$, D–W > 1.8. A runs test (Z_{run}) between −2 and +2 is considered acceptable.

Anisotropy decay data were fitted to a double-exponential function

$$r(t) = r_0 \sum_{i=1}^{2} g_i \exp(-t/\theta_i) \quad (4)$$

where θ_i are the two rotational correlation times with fractional amplitudes g_i, and r_0 is the limiting anisotropy at zero-time.

Chemicals and Reagents. Tris and EGTA were purchased from Sigma Chemicals (St. Louis, MO), and acrylamide (99.9%) was obtained from Bio-Rad Laboratories (Richmond, CA). All other chemicals were of reagent grade.

Results

Steady-State Spectrum and Quenching by Acrylamide. Upon excitation at 295 nm, the fluorescence emission spectrum of S-100a protein showed a peak at 330 nm at pH 7.5 and 335 nm at pH 8.5. The addition of Ca^{2+} resulted in a small red shift and increased quantum yield at both pH values (Table I). The fluorescence intensity was quenched in the presence of acrylamide, and the Stern–Volmer plots of the quenching data are shown in Figure 1. The data for both pH 7.5 and 8.5 were linear over a wide range of acrylamide concentration,

Table I: Steady-State Fluorescence Parameters of S-100a Protein at 20 °C[a]

pH	condition	λ_{em} (nm)	relative quantum yield	K_{sv} (M^{-1})
7.5	no Ca^{2+}	330	1.00	4.03 ± 0.03
	+ Ca^{2+}	333	1.40	4.29 ± 0.03
8.5	no Ca^{2+}	335	1.21	4.77 ● 0.09
	+ Ca^{2+}	337	1.52	5.47 ± 0.12

[a] Samples (≃10 μM) were excited at 295 nm for determination of λ_{em} and quantum yield, and duplicate samples were used for these determinations. The dynamic Stern–Volmer quenching constant (K_{sv}) was determined in the presence of an increasing concentration of acrylamide with excitation at 295 nm and emission at 350 nm. The uncertainties for K_{sv} were the standard errors at the 95% confidence level.

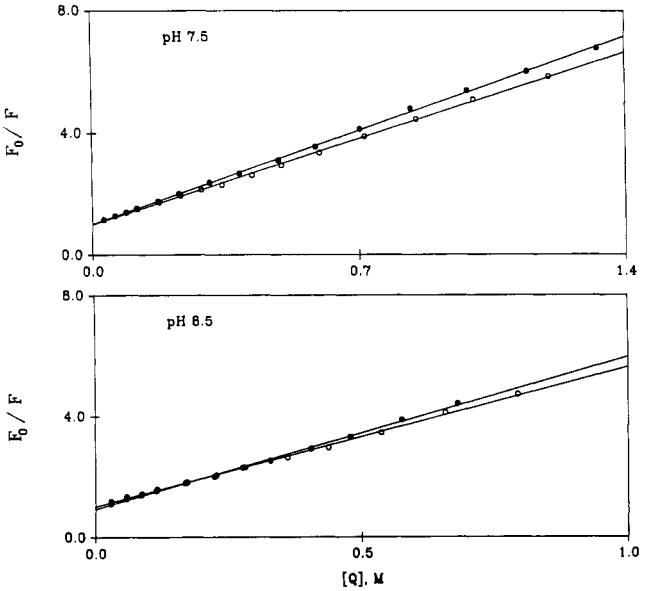

FIGURE 1: Stern–Volmer plots for the quenching of the fluorescence of S-100a protein by increasing concentration of acrylamide, [Q], at 20 °C and pH 7.5 and 8.5. F_0 is the fluorescence intensity measured at 350 nm with excitation at 295 nm in the absence of acrylamide, and F is the intensity measured in the presence of acrylamide. (○) Data obtained in the absence of Ca^{2+}; (●) in the presence of 2 mM Ca^{2+}.

suggesting the absence of static quenching. This was confirmed by fitting the data to eq 1. Ca^{2+} increased the slope of the plots, and its binding to the protein resulted in a small enhancement of the collisions between the tryptophan side chain and solvent molecules. When compared with pH 7.5, the alkaline pH also resulted in an enhanced solvent accessibility. The Stern–Volmer dynamic quenching constants are also listed in Table I. The increase in collisional quenching induced by Ca^{2+} and pH 8.5 was accompanied by a red spectral shift and an increased quantum yield. The spectral shift indicates a more polar/exposed environmnt consistent with the observed increased dynamic quenching by acrylamide. The reason for the observed increase in quantum yield is less obvious on the basis of steady-state data.

Fluorescence Intensity Decays. The intensity decays of S-100a were complex. A typical decay curve obtained at 360 nm with excitation at 300 nm is shown in Figure 2. A visual inspection of the two fits indicates that the data could not be fitted with a biexponential function, but the best fit was obtained with a triexponential function. Similar decay patterns were observed with 295-nm excitation and the emission isolated with a cut-off filter, regardless of pH, temperature, and solvent condition. The best decay parameters recovered at pH 7.2 for

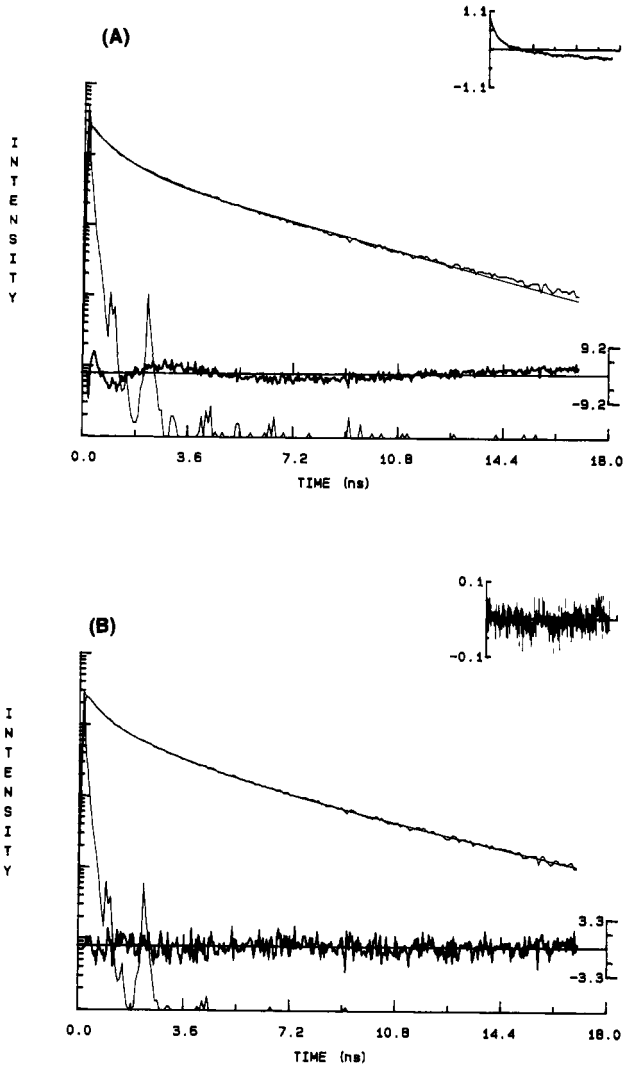

FIGURE 2: Fluorescence intensity decay of S-100a protein (≃10 μM) at pH 8.4. The excitation wavelength was 300 nm, and emission was isolated with a 360-nm interference filter. The sharp peak on the left is the lamp profile. The horizontal plot across the figure is the residual plot, and the inset at the upper right-hand corner is the autocorrelation function of the weighted residuals. The solid curve is the best-fitted curve convoluted with the lamp profile. (A) The decay data were fitted to a biexponential function with the following best-fitted decay parameters: $\alpha_1 = 0.71$, $\tau_1 = 0.81$ ns, $\alpha_2 = 0.29$, and $\tau_2 = 3.79$ ns. $\chi_R^2 = 3.55$, D–W = 0.55, and $Z_{run} = -3.82$. (B) The data were fitted to a triexponential function: $\alpha_1 = 0.55$, $\tau_1 = 0.43$ ns, $\alpha_2 = 0.31$, $\tau_2 = 1.70$ ns, $\alpha_3 = 0.14$, and $\tau_3 = 4.48$ ns. $\chi_R^2 = 1.00$, D–W = 2.02, and $Z_{run} = -0.12$.

both sets of emission conditions are given in Table II. In every case, the three lifetimes were well separated with any pair of lifetimes $\tau_{i+1}/\tau_i > 3$. In the majority of cases, the fractional contribution of each component was >10%. These results suggest that the resolution of the three-exponential decay was not problematic, and the goodness of the fits was supported by various statistical criteria.

At 20 °C and pH 7.2, the three lifetimes of the apoprotein measured at 360 nm were in the range of 0.42–4.73 ns with the associated fractional amplitudes (α_i) being 0.57, 0.31, and 0.12. The shortest component (α_1) contributed 57% to the total decay, whereas the longest component contributed 12%. When the decay was determined with the cut-off filter, the three lifetimes remained about the same, but the amplitudes changed to 0.68, 0.23, and 0.09. Under this emission condition, the relative populations of the three components shifted in favor of the shortest component at the expense of the two long components. Since the emission peak was at 330 nm, the

Table II: Fluorescence Intensity Decays of S-100a Protein at pH 7.2[a]

	°C	α_1	τ_1 (ns)	α_2	τ_2 (ns)	α_3	τ_3 (ns)	$\langle\tau\rangle$ (ns)	χ_R^2	D–W
no cation	20	0.68 (0.57)	0.43 (0.42)	0.23 (0.31)	1.24 (1.75)	0.09 (0.12)	4.05 (4.73)	2.04 (1.02)	1.13 (1.02)	1.91 (1.95)
	4	0.76	0.41	0.18	1.39	0.06	4.65	2.11	1.11	1.99
magnesium	20	0.75	0.44	0.19	1.46	0.07	4.48	2.11	1.02	2.00
	4	0.75	0.44	0.19	1.44	0.07	5.05	2.39	1.02	2.14
calcium	20	0.30 (0.44)	0.38 (0.43)	0.45 (0.39)	1.87 (1.70)	0.25 (0.17)	4.63 (5.01)	3.32 (3.24)	1.05 (1.04)	1.88 (1.98)
	4	0.39	0.32	0.37	1.69	0.24	4.95	3.60	1.01	1.67

[a] S-100a ($\simeq$10 μM) was in 25 mM Tris. The samples wee excitated at 295 nm, and the emission was isolated with a 0–54 cut-off filter. The results given in parentheses were obtained with excitation at 300 nm and emission isolated at 360 nm. The mean lifetime was calculated from $\langle\tau\rangle = \sum\alpha_i\tau_i^2/\sum\alpha_i\tau_i$. The standard errors were ~3% for α_i and ~2% for τ_i.

Table III: Fluorescence Intensity Decays of S-100a Protein at pH 8.2[a]

	°C	α_1	τ_1 (ns)	α_2	τ_2 (ns)	α_3	τ_3 (ns)	$\langle\tau\rangle$ (ns)	χ_R^2	D–W
no cation	20	0.72 (0.55)	0.40 (0.43)	0.20 (0.31)	1.26 (1.70)	0.07 (0.14)	4.06 (4.48)	1.95 (2.78)	1.05 (1.00)	2.07 (2.02)
	4	0.73	0.46	0.20	1.43	0.07	4.93	2.39	0.98	1.94
magnesium	20	0.68	0.38	0.24	1.20	0.08	4.42	2.26	1.00	1.99
	4	0.74	0.49	0.19	1.58	0.07	5.29	2.56	0.98	2.01
calcium	20	0.39 (0.40)	0.32 (0.45)	0.39 (0.40)	1.57 (1.98)	0.22 (0.20)	4.49 (5.19)	3.15 (3.57)	1.12 (0.97)	1.95 (2.10)
	4	0.35	0.37	0.35	1.68	0.30	5.03	3.97	1.01	1.97

[a] The samples were in 25 mM Tris, pH 8.2. The excitation wavelength was 295 nm, and the emission was isolated with a 0–54 cut-off filter. The results given in parentheses were obtained with samples in 25 mM Tris and pH 8.4, and these samples were excited at 300 nm with the emission isolated at 360 nm. Other conditions and the standard errors of the recovered parameters were the same as indicated in Table II.

emitted photons isolated by the cut-off filter were of a wide range of frequencies and had a higher average energy than those isolated at 360 nm. The differences in the amplitudes observed between the two emission conditions may be related to the difference in the energies of the two sets of detected photons.

The addition of Mg^{2+} did not alter the lifetimes much and increased α_1 by about 10%. However, Ca^{2+} induced substantial changes in the decay parameters. A significant change was observed in the amplitudes: α_1 decreasing from 0.68 to 0.30 and α_2 and α_3 increasing to 0.45 and 0.25, respectively. The contribution of the shortest decay component was reduced by a factor of 2.3 when the protein was saturated with Ca^{2+}. As a consequence of these changes, the mean lifetime was increased by 1.3 ns. Qualitatively, similar Ca^{2+}-induced changes were also observed when the decay was determined at 360 nm. When the temperature was lowered to 4 °C, the mean lifetimes generally increased. Similar Ca^{2+}-induced changes in the amplitudes of the three lifetimes were also observed at the lower temperature.

At pH 8.2 and 8.4, the decay parameters were comparable to those observed at pH 7.2, as shown in Table III. The shortest decay component of the apoprotein contributed 55% to the total decay when it was determined at 360 nm and increased to 72% when detected with a cut-off filter. Mg^{2+} had small effects on the amplitudes, but Ca^{2+} significantly reduced the amplitude of the shortest component regardless of the emission condition, as was observed at neutral pH. With the cut-off filter, Ca^{2+} reduced α_1 by a factor of 1.8 as compared with a factor of 2.3 at pH 7.2. Thus, there were no large differences in the decay properties between pH 7.2 and pH 8.2–8.4.

Anisotropy Decays. The anisotropy decay of the single Trp 90 of S-100a at pH 7.2 was biphasic, as shown in Figure 3. The fast component was characterized by a rotational correlation time (θ_1) of 1.09 ns and the slow component by a correlation time (θ_2) of 16.22 ns. About 39% of the recovered anisotropy r_0 was associated with the short component. The value of θ_1 probably was too slow to be attributed to unrestricted side-chain motions, but certainly reflected motions associated with the indole ring. The long correlation time provided a measure of the overall motion of the protein. The

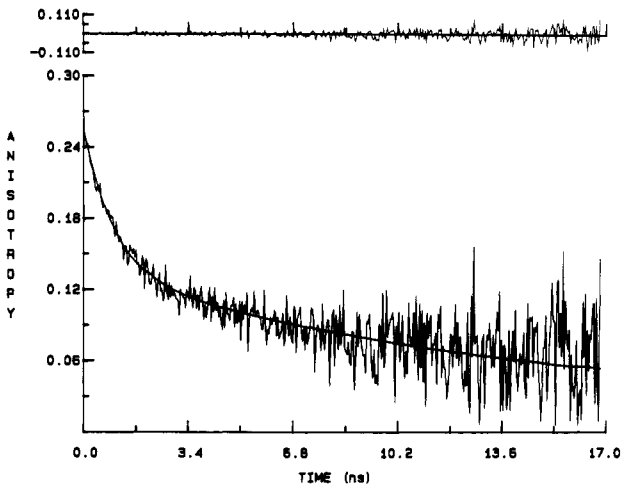

FIGURE 3: Representative fluorescence anisotropy decay curve for S-100a protein at 20 °C and pH 8.4. The excitation wavelength was 300 nm, and emission was isolated with a 360-nm interference filter. The decay data were fitted to a biexponential function with the following best-fitted decay parameters: $g_1r_0 = 0.131$, $\theta_1 = 1.04$ ns, $g_2r_0 = 0.125$, and $\theta_2 = 18.03$ ns. $\chi_R^2 = 1.04$, and D–W = 1.97.

addition of Ca^{2+} did not affect θ_1 much but decreased its contribution to the recovered anisotropy from 39 to 26%. Concomitantly, θ_2 was increased by 5.8 ns, suggesting a more asymmetric hydrodynamic shape for the Ca^{2+} complex. In both the apoprotein and the Ca^{2+} complex, the recovered anisotropy was much smaller than the value of 0.31 expected of immobilized tryptophan with excitation in the 270–300-nm range (Valeur & Weber, 1977; Ludescher et al., 1988). These results are given in Table IV together with the anisotropy results determined at pH 8.4. When compared with pH 7.2, the alkaline pH had only small effects on the apoprotein, increasing θ_2 by 2 ns and the contribution of the short component to 50% with no effect on r_0. The apoprotein at pH 8.4 had a slightly more asymmetric shape than at pH 7.2. A significant difference in the anisotropy decay between the two pH values was observed in the presence of Ca^{2+}. The short anisotropy component, which contributed 50% to the recovered anisotropy of the apoprotein, disappeared in the calcium complex at pH 8.4. The protein now appeared to tumble with

Table IV: Fluorescence Anisotropy Decays of S-100a Protein at 20 °C[a]

pH	condition	g_1r_0	θ_1 (ns)	g_2r_0	θ_2 (ns)	r_0	χ_R^2	D-W
7.2	no cation	0.103	1.09	0.153	16.22	0.261	1.17	2.03
	calcium	0.063	1.30	0.181	21.96	0.244	1.07	2.04
8.4	no cation	0.131	1.04	0.125	18.03	0.256	1.04	1.97
	calcium			0.221	16.38	0.221	1.16	2.03

[a] The anisotropy decays were measured with excitation at 300 nm, and the emission was isolated with a 360-nm interference filter. The zero time anisotropy r_0 is given by $r_0 = g_1r_0 + g_2r_0$, where g_1 and g_2 are the fractional amplitudes of the fast and slow decay components with respective rotational correlation times θ_1 and θ_2. The standard errors of the two correlation times were 5% or less.

a single correlation time of 16.38 ns. There are two possibilities for the disappearance of the short correlation time. One is that Ca^{2+} immobilized the tryptophan side chain so that the protein would tumble as a rigid molecule. The other possibility is an enhanced side-chain mobility, as suggested by the decrease of the zero-time anisotropy from 0.256 to 0.221. This reduction in r_0 suggests that Ca^{2+} binding may have resulted in the appearance of some very fast motion of the indole ring and this fast motion would be on a time scale outside the time window of the present experiment. To ascertain whether the value $r_0 = 0.221$ could be due to artifacts in the decay measurements, we carried out isothermal steady-state anisotropy measurements of the protein in the presence of Ca^{2+} under the same optical conditions as in the decay measurements. The limiting anisotropy extrapolated from the steady-state Perrin plot was 0.210, in agreement with decay measurements. It is clear that a change in pH from 7.2 to 8.4 produced only minor changes in the intensity decay properties of the Trp 90, but in this pH 8.4 conformation the residue in the Ca^{2+} complex appeared to experience some very fast picosecond motion which was not present at pH 7.2.

Discussion

We have investigated the emission properties of the single Trp 90 of the α-subunit in the $\alpha\beta$ dimer of S-100a protein. The steady-state Stern–Volmer plots have yielded dynamic acylamide quenching constants in the range of 4.03–5.47 M^{-1}. The extent of the exposure of the Trp 90 to solvent under different conditions can be ordered as follows: pH 7.5 < pH 7.5 + Ca^{2+} < pH 8.5 < pH 8.5 + Ca^{2+}. Although the protein has three tyrosyl residues, the quenching results reflect the properties of the single tryptophan residue because the excitation wavelength was 295 nm. The K_{SV} values for single-tryptophan peptides and proteins range from 10–13 M^{-1} for a fully exposed residue to less than 1 M^{-1} for a fully buried residue (Eftink & Ghiron, 1976). On this basis, the single Trp 90 in the $\alpha\beta$ dimer is partially buried and not likely on the protein surface. The emission maximum of 330 nm for the apoprotein is consistent with the K_{SV} value. The calcium binding renders the residue more acessible to acrylamide quenching at both pH values, and in this environment the residue is more exposed to solvent relative to in the apoprotein. The environment of the tryptophan in the calcium complex at pH 8.5 is the most polar, but in that environment the residue is still far from being fully exposed to the aqueous solvent because K_{SV} is still relatively small. The surface probability (Emini et al., 1985) of the Trp 90 is predicted to be very low (0.675), consistent with a small K_{SV}. As a comparison, the single tryptophan of cardiac troponin I has a predicted surface probability of 11.7, and the K_{SV} of acrylamide quenching for this residue is 10.1 (Liao et al., 1992), both results consistent with a highly exposed residue. The short rotational correlation time (which will be discussed later) is on the order of 1 ns both in the absence and presence of Ca^{2+} and at neutral or a slightly alkaline pH. This 1-ns correlation time is not compatible with a freely rotating indole ring, but compatible with a side chain which experiences restricted motional freedom. The restricted motion may reflect either a segmental motion of the polypeptide chain or interaction of the indole ring with the side chains of adjacent residues. When taken together, these results suggest that Trp 90 is partially buried in the apoprotein. An alkaline pH or the presence Ca^{2+} results in a small increased exposure of the residue to the solvent, and the Ca^{2+}-induced exposure is slightly larger at pH 8.5 than at pH 7.5. This exposure, however, is not sufficient to move the residue to the protein surface. In a previous study of Ca^{2+}-induced UV-difference spectra of S-100a, Mani and Kay (1983) reported $\Delta\epsilon$ values at 292.5 nm of −460 and −330 at pH 8.3 and 7.5, respectively, indicating that the tryptophan residue is relatively more exposed in the Ca^{2+} complex at a given pH. Since $\Delta\epsilon = -1600$ for a fully exposed tryptophan (Donovan, 1969), the results from UV-difference spectra are in agreement with the present conclusion that the Trp 90 in the $\alpha\beta$ dimer is partially buried in both the apoprotein and its calcium complex.

The complexity of the intensity decays is somewhat surprising because the steady-state Stern–Volmer plots show no downward curvature to suggest emission heterogeneity. The same decay patterns were observed using two different picosecond fluorometers, and this agreement provides confidence in our conclusion of a triexponential model for the intensity decay of the protein. While many single-tryptophan proteins exhibit multiple exponential decays (Chen et al., 1987; Hutnik & Szabo, 1989; Liao et al., 1992), the underlying mechanisms for the emission heterogeneity are different for different proteins. Both ground-state and excited-state interactions can give rise to multiplicity in intensity decay. In the absence of crystallographic or other type of spectroscopic information, it is difficult to discuss the possible origin of the observed multiple decays in terms of specific interactions and different rotamers with respect to different C–C bonds. The secondary structure of the α-subunit predicted by the methods of CF (Chou & Fasman, 1976) and GOR (Garnier et al., 1976), using the algorithm of the University of Wisconsin Genetics Group, locates the Trp 90 in a segment that is either a β-turn (GOR) or at the end of a β-sheet followed by residues with β-turn characteristics (CF). There may be transient interactions between the indole ring and adjacent side chains. In particular, an interaction between the carboxylate group of Glu 91 and the side chain of Trp 90 could result in destabilization of the excited-state indole ring. Such a destabilization was previously demonstrated with model compounds (Szabo & Rayner, 1980) and would lead to fluorescence emission with a shorter time constant and at higher energies. Since the indole ring rotates rapidly during the excited-state lifetime (as evidenced from anisotropy decay results), the putative interaction can change during this time interval, and this could result in complex decay patterns. Thus, the decay component that is related to the excited-state interaction is expected to be more dominant at a shorter wavelength. We have shown that the three lifetimes of S-100a are not sensitive to the emission wavelength at which the decay is measured. On the other hand, the proportions of these decay components are sensitive

to emission wavelength. The fraction of the shortest component (α_1) is higher in the blue end of the emission spectrum than in the red region as indicated by the different values of α_1 obtained with the cut-off filter and at 360 nm. These results are consistent with our suggestion of an interaction between Glu 91 and Trp 90, and this interaction may, at least in part, be responsible for the shortest lifetime.

The conformational change induced by Mg^{2+} in the Trp 90 environment is very minimal. The longer mean lifetime observed in the presence of Ca^{2+} is in agreement with an enhanced quantum yield. The significant result is that, upon binding Ca^{2+}, α_1 is reduced by a factor of 2.3. The same qualitative change in α_1 is observed at pH 8.2 and in the red region of the emission spectrum at both neutral and alkaline pH. We suggest that the Ca^{2+} binding significantly reduces the Trp 90–Glu 91 interaction, resulting in a large decrease in the proportion of the shortest decay component. From comparison of protein sequences with troponin C and parvalbumin, a 12-residue segment (residues 62–73) was identified in the α-subunit as a potential Ca^{2+}-binding loop (Isobe & Okuyama, 1981). The segments flanking the loop are predicted by GOR to be α-helical, from residues 46–61 and 74–84. If the properties of this loop are similar to those of the other Ca^{2+}-binding proteins, the binding should induce the helix–loop–helix motif to adopt an EF hand that is characteristic of the Ca^{2+}-saturated helix–loop–helix motif. The formation of an EF hand with bound Ca^{2+} would require reorientations of the two flanking helical segments, as suggested by modeling studies of the Ca^{2+}-binding sites in the N-domain of troponin C (Herzberg et al., 1986). These reorientations may in turn perturb the Trp 90–Glu 91 interaction and be the molecular origin of the decreased population of the shortest decay component. A consequence of the disruption of the destabilization of the excited-state indole ring is an increase in the weighted mean lifetime and quantum yield. These predicted changes have been observed in the presence of 2 mM Ca^{2+}.

A previous study reported biexponential intensity decays for S-100a with lifetimes of 0.65 and 2.6 ns at pH 7.1 and associated fractional amplitudes of 0.42 and 0.57, respectively (Baudier et al., 1984). In the presence of Ca^{2+}, their lifetimes were 0.9 and 3.0 ns with respective amplitudes 0.12 and 0.88. There is an apparent disagreement between the previous results and the present work on the number of exponential terms that must be used to describe the decay satisfactorily. Our triexponential model was established from data collected with two different instruments, and the data were evaluated by several statistical parameters. These parameters clearly show that a biexponential function is unacceptable for the present data. It is unclear to what extent the previous data could be fitted to a different decay model. We note that the weighted mean lifetime from the previous biexponential fits was 2.3 ns in the absence of Ca^{2+} and 2.9 ns in the presence of Ca^{2+}. The proportion of the short component was significantly reduced by the presence of Ca^{2+}, as we have observed for the shortest decay component in the present work. The properties of the previous short component would suggest that it may correspond to the present shortest component or a combination of the two shortest components. Baudier et al. (1984) suggested the presence of internal dynamic quenching of the Trp 90 emission in the apoprotein and removal of this quenching by Ca^{2+} binding. We have discussed the emission heterogeneity in terms of a plausible excited-state interaction which is supported by current knowledge of the spectroscopic properties of the interaction.

The long rotational correlation time observed at pH 7.2 for the apoprotein is considerably longer than that for a spherical protein with any reasonable degree of hydration. If the protein is approximated by a revolution of prolate ellipsoid, the harmonic mean of the two rotational correlation times (θ_h) can be readily calculated using appropriate frictional coefficients (Keoing, 1975) for various axial ratios. Comparison of these harmonic mean values with the observed long correlation time (θ_2) provides a measure of the hydrodynamic shape of the protein. We used a value of 0.707 cm^3/g for the partial specific volume (Mani & Kay, 1984) and hydration values ranging from 0 to 0.5 g of water/g of protein in the calculation of θ_h. The results show that a θ_2 value of 16 ns is compatible with an axial ratio in the range of 4–5 and a hydration of 0.2–0.3. An increase of 5–6 ns in θ_2 would change the axial ratio to the range of 5–6 if the hydration remains unchanged. A change of pH from 7.2 to 8.4 causes only a small increase in the axial ratio of the apoprotein, certainly less than that caused by Ca^{2+} at pH 7.2. The asymmetric shape of S-100a demonstrated here is in agreement with previously reported hydrodynamic results by Mani and Kay (1984). In addition, the alkaline pH increases the fractional contribution of the short anisotropy component to the total anisotropy in the apoprotein, whereas Ca^{2+} decreases this contribution at pH 7.2. From the anisotropies recovered for the two decay components, the half-angle of a cone traversed by the tryptophan side chain is 32° in the apoprotein and 25° in the Ca^{2+} complex at pH 7.2, indicating a smaller amplitude in the side-chain motion in the complex. This more restricted motion must result from changes in the immediate secondary/tertiary structure surrounding the residue and is consistent with our interpretation of the observed decrease in α_1. While this new environment is more restricted, it is slightly more accessible to solvent as the tryptophan fluorescence in the Ca^{2+} complex is more quenched than in the apoprotein. On the other hand, pH 8.4 increases the half-angle of the cone to 38°, and this larger amplitude would suggest a more open environment which is also more accessible to solvent molecules than at pH 7.2. Another indication of a difference in the S-100a conformation between the two pH values is the apparent absence of a fast anisotropy decay component for the Ca^{2+} complex at pH 8.4. As has been pointed out, the disappearance of the fast anisotropy component does not necessarily suggest an immobilized tryptophan side chain. It appears that there may be other modes of very fast side-chain motion generated by Ca^{2+} at pH 8.4 and not resolvable. The instrument used for these measurements had a time resolution of 60–70 ps. Thus, the unresolved fast motion must be faster than 100 ps and occur in an environment that is moderately polar but unlikely the protein surface. Taken together, the time-resolved fluorescence results indicate substantial differences in both the local and global conformations of S-100a at the two pH values. These differences may be related to the difference in the number of Ca^{2+}-binding sites at pH 7.5 and 8.4 that were determined by intrinsic fluorescence (Mani & Kay, 1983) and to the titration of a histadine residue in the β-subunit (Mani et al., 1983). The present results do not provide an indication as to whether the residue is located within the tertiary structure of the α-subunit or in a contact region between the α- and β-subunits. In the absence of this information, the observed Ca^{2+} effect may be related to changes in either the α-subunit conformation or the quaternary structure.

In conclusion, the fluorescence intensity decay of the single Trp 90 of the α-subunit in the dimeric structure of S-100a protein is complex. One of the three resolved components may

arise from a specific interaction between the indole ring and the side chain of an adjacent residue. Ca^{2+} binding to a site located at the C-terminal half may result in reorientations of the flanking helical segments leading to formation of a putative EF hand and hence disruption of the interaction between the tryptophan side chain and an adjacent side chain. Qualitatively similar changes are observed in the steady-state fluorescence spectrum induced by Ca^{2+} at pH 7.2 and by changing the pH from 7.2 to 8.4 in the absence of Ca^{2+}. However, there are subtle differences between the conformations of Ca^{2+}-bound S-100a at neutral pH and the apoprotein at pH 8.4.

ACKNOWLEDGMENTS

We thank Professor Bruce Hudson for permission to use his picosecond fluorometer for several of the experiments reported in this work. We are indebted to Dr. Ian Johnson for expert assistance in using the picosecond instrument and the analysis software at the University of Oregon.

Registry No. Trp, 73-22-3; Ca, 7440-70-2; Mg, 7439-95-4.

REFERENCES

Baudier, J., Tyrzk, J., Lofroth, J. E., & Lianow, P. (1984) *Biochem. Biophys. Res. Commun. 123*, 959–965.

Baudier, J., Glasser, N., & Duportail, G. (1986) *Biochemistry 25*, 6934–6941.

Chen, L. X.-Q., Longworth, J. W., & Fleming, G. R. (1987) *Biophys. J. 51*, 865–873.

Chou, P. Y., & Fasman, G. D. (1978) *Annu. Rev. Biochem. 47*, 251–276.

Cocchia, D., Michetti, F., & Donato, R. (1981) *Nature (London) 294*, 85–87.

Donovan, J. W. (1969) in *Physical Principles and Techniques in Protein Chemistry* (Leach, S. J., Ed.) Part A, pp 101–170, Academic Press, New York.

Durbin, J., & Watson, G. S. (1951) *Biometrika 38*, 159–178.

Eftink, M. R., & Ghiron, C. A. (1976) *Biochemistry 15*, 672–680.

Emini, E. A., Hughes, J. V., Perlow, D. S., & Boger, J. (1985) *J. Virol. 55*, 836–839.

Garnier, J., Osguthrope, D. J., & Robson, B. (1978) *J. Mol. Biol. 120*, 97–112.

Grinvald, A., & Steinberg, I. Z. (1974) *Anal. Biochem. 59*, 583–598.

Gunst, R. F., & Mason, R. L. (1980) in *Regression Analysis and Its Applications*, pp 232–234, Marcel Dekker, New York.

Herzberg, O., Moult, J., & James, M. N. G. (1986) *J. Biol. Chem. 261*, 2638–2644.

Hutnik, C. M., & Szabo, A. G. (1989) *Biochemistry 28*, 3923–3934.

Isobe, T., & Okuyama, T. (1978) *Eur. J. Biochem. 89*, 379–388.

Isobe, T., & Okuyama, T. (1981) *Eur. J. Biochem. 116*, 79–86.

Isobe, T., Nakajima, T. Y., & Okuyama, T. (1977) *Biochim. Biophys. Acta 494*, 222–232.

Kanamori, M., Endo, T., Shirakawa, S., Sakurai, M., & Hidaka, H. (1982) *Biochem. Biophys. Res. Commun. 108*, 1447–1453.

Koeing, S. (1975) *Biopolymers 14*, 2421–2423.

Lampert, R. A. L., Chewter, L. A., Phillips, D., O'Connor, D. V., Roberts, A. J., & Meech, S. R. (1983) *Anal. Chem. 55*, 68–73.

Liao, R., Wang, C.-K., & Cheung, H. C. (1992) *Biophys. J.* (in press).

Ludescher, R. D., Johnson, I. D., Volverk, J. J., de Hass, G. H., Jost, P. C., & Hudson, B. S. (1988) *Biochemistry 27*, 6618–6628.

Ludwin, S. K., Kosek, J. C., & Eng, L. F. (1976) *J. Comp. Neurol. 165*, 197–208.

Mani, R. S., Boyes, B. E., & Kay, C. M. (1982) *Biochemistry 21*, 2607–2612.

Mani, R. S., & Kay, C. M. (1983) *Biochemistry 22*, 3902–3907.

Mani, R. S., & Kay, C. M. (1984) *FEBS Lett. 166*, 258–262.

Mani, R. S., & Kay, C. M. (1985) *FEBS Lett. 181*, 275–280.

Mani, R. S., & Kay, C. M. (1987) *Methods Enzymol. 139*, 168–187.

Mani, R. S., Shelling, J. G., Sykes, B. D., & Kay, C. M. (1983) *Biochemistry 22*, 1734–1740.

Marquardt, D. W. (1963) *J. Soc. Ind. Appl. Math. 11*, 431–441.

Moore, B. W. (1965) *Biochem. Biophys. Res. Commun. 6*, 739–44.

Moore, B. W. (1973) *Proteins of the Nervous System* (Schneider, D. J., Ed.) p 1, Raven Press, New York.

O'Connor, D. V., & Phillips, D. (1984) *Time-Correlated Single Photon Counting*, Academic Press, London.

Ruggiero, A., & Hudson, B. (1989) *Biophys. J. 55*, 1111–1124.

Stefansson, K., Wollmann, R. L., Moore, B. W., & Arnason, B. G. W. (1982) *Nature (London) 295*, 63–64.

Szabo, A. G., & Rayner, D. M. (1980) *J. Am. Chem. Soc. 102*, 554–563.

Szebenyi, D. M. E., Obendorf, S. K., & Moffat, K. (1981) *Nature (London) 294*, 327–332.

Tufty, R. M., & Kretsinger, R. H. (1975) *Science 187*, 167–169.

Valeur, B., & Weber, G. (1977) *Photochem. Photobiol. 25*, 441–444.